Letter

Room-temperature transparent oxide spin electronics: A conducting interface in LaFeO₃−SrTiO₃

Ripudaman Kaur,[1,2,*] Anamika Kumari,[1,*] Shinjini Paul,[3] Mohd Anas,[4] Bibek Ranjan Satapathy,[1] Sanjeev Kumar,[2]
V. K. Malik,[4] P. Mahadevan,[3] D. D. Sarma,[5,6] and Suvankar Chakraverty [1,†]

[1]*Quantum Materials and Devices Unit, Institute of Nano Science and Technology, Mohali, Punjab 140306, India*
[2]*Applied Science Department, Punjab Engineering College (Deemed to be University), Sector-12, Chandigarh 160012, India*
[3]*S. N. Bose National Centre for Basic Sciences, Kolkata, West Bengal 700106, India*
[4]*Department of Physics, Indian Institute of Technology Roorkee, Roorkee 247667, India*
[5]*CSIR-National Institute for Interdisciplinary Science and Technology (CSIR-NIIST),*
Industrial Estate P.O., Pappanamcode, Thiruvananthapuram 695019, India
[6]*Solid State and Structural Chemistry Unit, Indian Institute of Science Bengaluru, Karnataka 560012, India*

The quest for realizing highly spin-polarized conduction in materials at room temperature is one of the central themes of materials physics. We report on the realization of a conducting interface in LaFeO₃ (LFO)-SrTiO₃ (STO) that demonstrates spin-polarization signatures, namely, negative magnetoresistance (MR) and anomalous Hall resistivity >150 K and even up to room temperature. However, the same system shows positive MR and normal Hall effect at temperatures <150 K. From density functional theory calculations, we find that this is related to the structural transition of the substrate, amplified here as the changes happen at the interface. This leads to a net spin polarization of the interface states at the Fermi energy in the high-temperature phase, allowing for an anomalous Hall effect and negative MR. In addition, this interface appears to be almost transparent in the entire range of visible light. Our observation might be viewed as a step toward room-temperature transparent oxide spintronics.

The application of a magnetic field changes both the longitudinal and transverse resistance of the conductor [1–3]. In usual nonmagnetic metals, longitudinal resistance increases as a quadratic function of the applied magnetic field [positive magnetoresistance (MR)] and transverse resistance as a linear function of the applied magnetic field (normal Hall Effect). In several instances, these expectations are not met due to the presence of nontrivial topology of the band structure in the momentum space or nontrivial spin texture in real space. A few instances of such unusual occurrences of longitudinal and transverse MR are negative MR [4], anisotropic MR [5], singular MR [6], anomalous Hall effect [7], topological Hall effect [8], and quantum Hall effect [9]. Understanding and controlling such uncommon MRs is important in fundamental physics and spintronic devices that exploit the electronic spin for manipulating charge transport [1,10]. A convenient way to realize such physical systems is through interfaces of two distinct materials or superlattices. An era of oxide electronics has emerged after the realization of the two-dimensional electron gas (2DEG) at the interfaces between two insulating oxides LaAlO₃ (LAO) and SrTiO₃ (STO) [11]. This interface paves the way for the field of spintronics because, unlike conventional 2DEGs, this 2DEG consists of electrons with 3*d* character, thus leading to the possibility of incorporating magnetic interaction [12]. Unusual MRs such as anomalous

Hall effect, negative MR, and magnetization have been reported in this interface, but they are typically weak and observed at very low temperatures [5,13]. There have been multiple reports of perovskite oxide-based magnetic metals being deposited on STO, which exhibit anomalous Hall effects, namely, CaRuO₃ and SrRuO₃ [14,15]. Furthermore, researchers have observed a nonlinear Hall Effect at the conducting interfaces based on STO, such as LaTiO₃/SrTiO₃ and LaVO₃/SrTiO₃ appearing at low temperatures [16,17]. These nonlinear Hall effects have been explained using a two-band model. However, to date, no conducting interface based on STO has been reported that simultaneously demonstrates the existence of negative MR and anomalous Hall effect. The increased desire for electronics that respond faster, are more efficient, and have more storage space stimulates the quest for materials. Transparent oxide spintronics is a field of research that focuses on the use of transparent oxides in spintronics devices. Spintronics is a branch of electronics that uses the spin of electrons to store and manipulate information, instead of their charge. Transparent oxides are materials characterized by optical transparency, making them suitable for integration with optoelectronic devices. If these materials exhibit not only optical transparency but also nontrivial electronic and magnetic properties, they could emerge as promising candidates for application in transparent spintronics. Transparent spin electronics aims to develop devices that can be integrated with optoelectronic devices, such as light emitting diodes (LEDs), solar cells, memory, displays, and transparent sensors. The transparency of sensors allows

---

*These authors contributed equally to this work.
†suvankar.chakraverty@gmail.com

monitoring of real-time data in a noninvasive way. In this letter, our objective is to realize optically transparent materials that exhibit intriguing magnetotransport properties at room temperature. Among other potential candidates, we have chosen LFO for this letter because of its high Néel temperature (740 °C) and interesting magnetic interdomain coupling [18,19]. The formation of the metallic interface at the LFO-STO heterostructure has been reported [20,21], but detailed magnetotransport measurement of this metallic interface especially near room temperature is still not explored. The proposed models in the literature for the origin of metallicity at the interface of LAO-STO are electronic reconstruction, cation intermixing, oxygen vacancy, and structural disorder. Among them, the most accepted model is electronic reconstruction, but in the case of LFO-STO, emphasis on cation intermixing/dynamic layer rearrangement is also suggested as a possible origin of the conducting interface [21].

The conducting electrons possess a Ti $3d$ character in the LAO-STO interface. On the other hand, it has already been reported that, unlike the LAO-STO interface, for the LFO-STO interface, the conduction electrons predominantly occupy the Fe $3d$ band because the Fe band lies below the Ti band owing to the band gaps and band alignments of STO and LFO [22,23]. This Fe band character of the conducting electrons might capture the essence of the magnetic spin texture of the LFO layer and might be reflected in the magnetotransport properties of the 2DEG formed at the interface of LFO-STO.

Here, we report on the appearance of room-temperature negative MR and anomalous Hall effect because of room-temperature spin-polarized conduction electrons at the conducting interface of LFO-STO. The negative MR and anomalous Hall effect convert into positive MR and normal Hall effect <150 K. Density functional theory calculations suggest that this is associated with the structural transition of the substrate. While the carriers at the Fermi level are not spin-polarized in the lower temperature regime when the substrate has tetragonal symmetry, they are found to be spin-polarized in the interfacial Ti layer, with a moment in the z direction in the high-temperature cubic phase of the substrate. Around 90% transparency has been observed for this interface in the visible and near-infrared (NIR) light region. Through controlled experiments, we have demonstrated that this is a unique feature of this interface at a low charge carrier density limit.

The thin film fabrication and surface characterization are discussed in Sec. 1 in the Supplemental Material [24]. In Fig. 1(a), we have drawn a schematic of the LFO-STO heterostructure and the layered arrangement of LFO and STO in the (001) direction. For transport measurements, the contacts were made with a wire bonder (West Bond, 7400 series) using Al wire. Transport measurements were carried out using a physical property measurement system (PPMS, 14 T Quantum Design Dynacool). The optical transmission measurements for the LFO-STO system were performed using an Agilent Carey UV-visible spectrometer. The sheet resistance of the sample as a function of the temperature is presented in Fig. 1(b). The resistance decreases with decreasing temperature down to 1.8 K, suggesting a metallic nature of the interface.
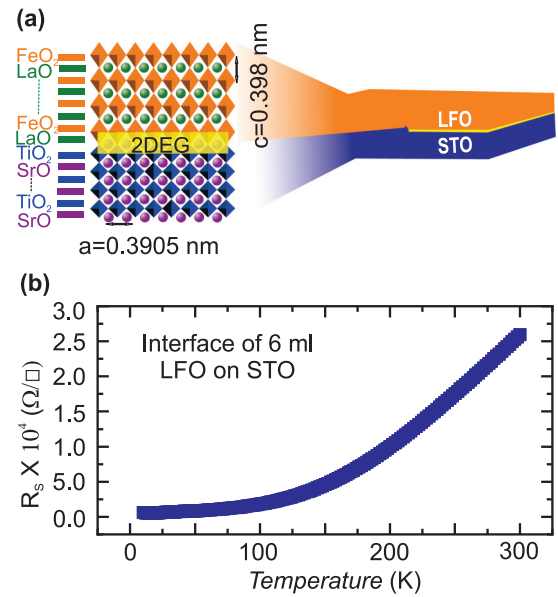

FIG. 1. Schematic and resistivity measurements. (a) Schematic of the LFO-STO heterostructure showing alternately charged layers arrangement in both LFO and STO that leads to the formation of the two-dimensional electron gas (2DEG) at the interface. (b) Temperature-dependent 2D resistivity of LFO-STO interface.

Figures 2(a) and 2(b) show the dependence of the percent MR (right axis) and Hall resistance (left axis) as functions of the applied magnetic field at 100 and 300 K, respectively. The percent MR is defined as $[\frac{R_{xx}(B)-R_{xx}(0)}{R_{xx}(0)}] \times 100$, where $R_{xx}(B)$ is the resistance at the magnetic field B, and $R_{xx}(0)$ is the resistance at zero magnetic field.

At 300 K [Fig. 2(b)], we have observed the signature of negative MR (1%) and nonlinear Hall resistance (a feature of the anomalous Hall effect), indicating the existence of an anomalous Hall effect. However, at 100 K, we have observed positive MR and linear Hall resistance as a function of B. Figures 2(c) and 2(d) show the raw Hall data (black) marked as R_{xy} as a function of the applied magnetic field, the linear fit (red) of the raw data, and the subtracted part (blue) of the raw data from the linear fit marked as anomalous Hall resistance (R_{xy}^{AHE}) for the LFO-STO interface at 100 and 300 K, respectively. To extract the anomalous component of the Hall data, we conducted a linear fitting within the magnetic field range of 10–14 T. Importantly, this same fitting procedure was applied to all Hall datasets to isolate the anomalous part. At 100 K, there is no signature of anomalous Hall resistance, whereas at 300 K, there is a finite anomalous Hall resistance. To avoid potential ambiguity arising from the subtraction process of the anomalous part of the Hall data with respect to temperature, we have depicted the difference in slopes at 13 and 3 T (the difference zero suggest the ordinary Hall effect and the finite difference suggests an anomalous Hall effect) as a function of temperature in Fig. S4 in the Supplemental Material [24]. This indicates strong agreement between the transition temperature derived from this method and that obtained through linear subtraction of the Hall data. To explore the transition from negative MR to positive MR and anomalous Hall effect to normal Hall effect at a low temperature further, we have
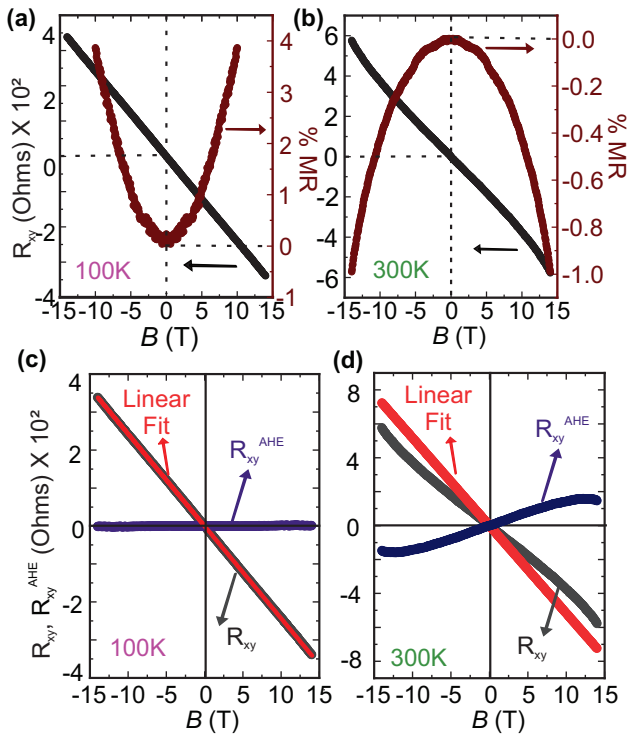
FIG. 2. Magnetotransport measurements at 300 and 100 K. (a) and (b) % magnetoresistance (right axis) and Hall resistance (left axis) as a function of the temperature of the LFO-STO interface measured at 100 and 300 K, respectively. (c) and (d) Raw Hall data (black) marked as R_{xy} as a function of the applied magnetic field, the linear fit (red) of the raw data, and the subtracted part (blue) of the raw data from the linear fit marked as anomalous Hall resistance (R_{xy}^{AHE}) for LFO-STO interface at 100 and 300 K, respectively.

performed longitudinal MR and transverse MR (R_{xy}) measurements at several selected temperatures.

Figures 3(a) and 3(b) depict the longitudinal percent MR and anomalous Hall effect as a function of the applied magnetic field measured at the selected temperatures. Figure 3(c) exhibits the magnetization as a function of the temperature measured under the application of a 100 Oe magnetic field. There are two important points to be noted from this figure. First, the magnetization is sustained even up to room temperature, and second, there is some phase transition at ∼150 K. It is evident that, <150 K, there is a rapid increase in magnetization as a function of the decreasing temperature. On the other hand, >150 K, the magnetization decreases rather slowly with increasing temperature. We call the low-temperature magnetic phase the x phase (<150 K) and the high-temperature phase the y phase. The detail of these two magnetic phases is not clear at this moment and needs further study, but at the same time, this is beyond the scope of this letter. The magnetization vs applied magnetic field data measured at 100 and 300 K are shown in Fig. S2 in the Supplemental Material [24]. The saturation magnetization at 300 K is lower than that at 100 K. We have performed M-T measurements on various samples with different thicknesses of LFO, and we have included the corresponding data in Fig. S3 in the Supplemental Material [24]. The obtained results indicate that the transition takes

place at ∼150 K for lower thickness and gradually disappears as the thickness of LFO increases. This finding aligns well with our nonlinear Hall and negative MR data (Fig. 4), which were obtained as a function of LFO film thickness. Figure 3(d) represents the percent MR (left axis) and anomalous Hall effect (right axis) as a function of temperature. It is worth noting that a positive to negative percent MR and nonzero anomalous Hall effect both appear >150 K. This correlation is remarkable and suggests that the high-temperature y-phase magnetic state is responsible for negative MR and nonzero anomalous Hall effect. We have considered three layers of $LaFeO_3$ grown on four layers of $SrTiO_3$ considering both the tetragonal (low temperature) and cubic (high temperature) phases [25] and calculated the electronic structure. The surface FeO_2 layer has an oxygen vacancy. Despite considering an antiferromagnetic arrangement of the Fe spins in each layer, a net magnetization develops in the presence of spin-orbit interactions and is larger in the tetragonal case than in the cubic case. The density of states (DOS) for the interfacial Fe (represented by the blue line) and Ti (represented by the red line) d orbitals is plotted in Fig. 3(e). The panels to the left of the dotted line correspond to the low-temperature phase, while those on the right represent the high-temperature phase. Additionally, the respective spin-polarized DOS for the interfacial Ti d states are also shown in each case. Based on these results, we associate the 150 K transition seen here to the tetragonal-to-cubic transition found in $SrTiO_3$, with its temperature increased because of the electron doping, as reported earlier [26]. The presence of oxygen vacancies in the surface layer leads to a partial occupancy of the interfacial Ti states, leading to their spin polarization for the cubic substrate, with the moment in the z direction. The spin polarization of the carriers at the Fermi level is found to vanish for the tetragonal substrate. These results are consistent with the experimental observations of the anomalous Hall effect, and the negative MR that one finds >150 K. As the interface plays an important role in the observed phenomena, the effects are associated with the phase transition of $SrTiO_3$. The Ti states at the Fermi level are found to have d_{xy} character, with small weights from the d_{xz} and d_{yz} orbitals. These orbitals couple with those on the neighboring oxygens as well as the interfacial Fe atoms leading to a small spread of the spin-polarized charge density onto those layers. Even in the tetragonal case that has no spin polarization at the Fermi level, by artificially changing the in-plane lattice parameter with a 1% expansion, one finds spin polarization developing with a slight narrowing of the bands. This suggests a Stoner mechanism for the observed spin polarization.

Figures 4(a) and 4(b) represent the percent MR and Hall resistance for the LFO-STO sample for different thicknesses of LFO film at room temperature as a function of B. It is observed that, with an increasing thickness of the LFO thin film, both the negative percent MR and the anomalous part [inset of Fig. 4(b)] of the Hall resistance decrease. We have calculated the carrier density of the samples with different thicknesses of the LFO layer from the high field slope of the Hall resistance. We have observed that, with an increasing thickness of the LFO layer, the carrier density initially increases rapidly, and then it slowly saturates. In Fig. 4(c), we have plotted the percent MR (left axis) and anomalous Hall resistance (right axis)
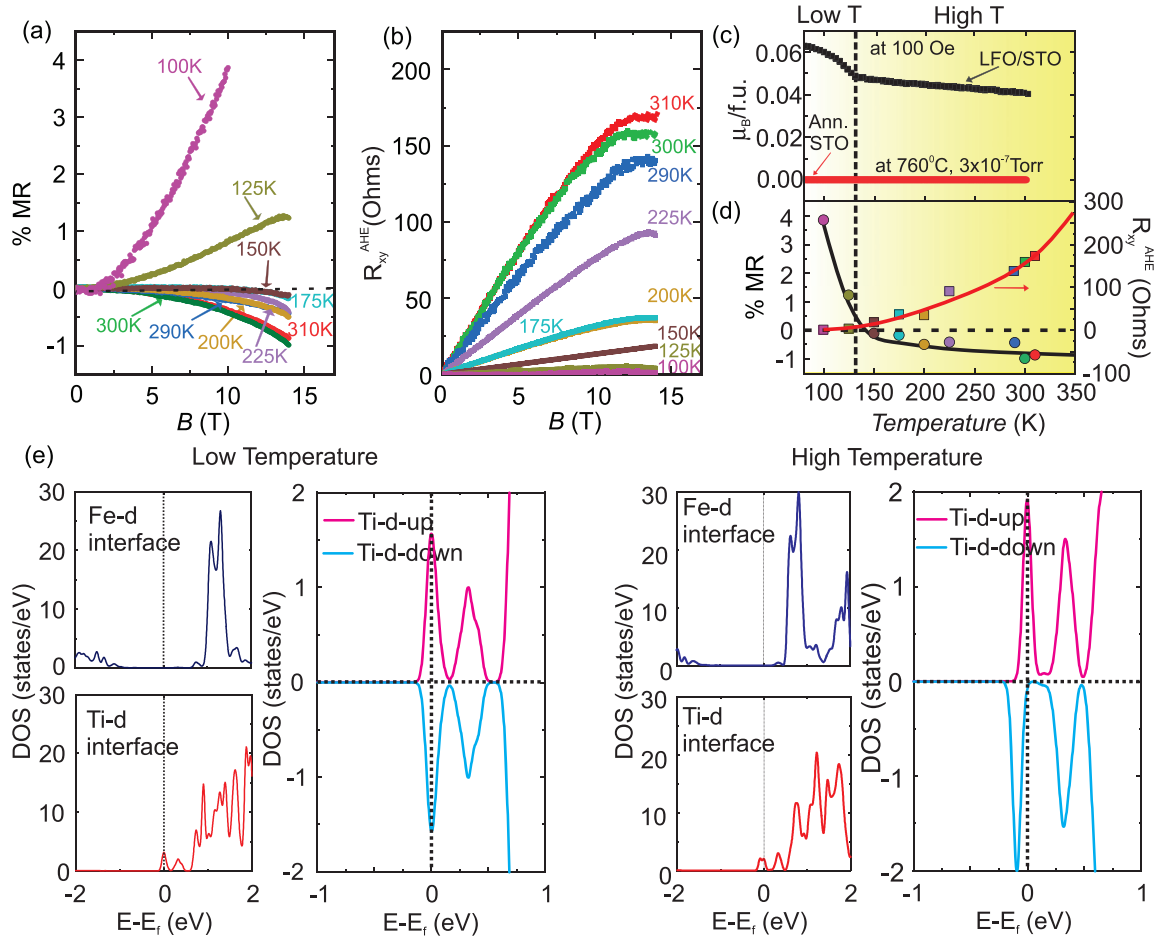
FIG. 3. Temperature-dependent magnetotransport and superconducting quantum interference device (SQUID) measurements. (a) Magnetoresistance (MR) of the LFO-STO interface as a function of the applied magnetic field measured at selected temperatures as marked in the figure. (b) Anomalous Hall resistance of the LFO-STO interface as a function of the applied magnetic field measured at selected temperatures as marked in the figure. (c) Magnetization of LFO-STO (black) and annealed STO (red) as a function of temperature measured under the application of 100 Oe magnetic field. (d) % MR (left axis) and anomalous Hall resistance (right axis) as a function of the temperature of the 6 ml LFO-STO interface. (e) The density of states (DOS), for the interfacial Fe (in Navy line) and Ti (in red line) d orbital, is plotted along with the spin-polarized DOS (m_z contribution of d orbital) of the interfacial Ti (up in pink line and down in blue line) for both when the substrate is in low temperature (tetragonal phase) and in high temperature (cubic phase).

as functions of carrier density. It is evident from this figure that an increasing carrier density decreases both negative MR and anomalous Hall resistance. To present a correspondence between the number of LFO layers and carrier density, we have marked the number of LFO layers at the top x axis. In STO, there is a band insulating gap of 3.2 eV between the O $2p$ and Ti $3d$ bands, and LFO is a charge transfer insulator with a band gap of 2.2 eV between the O $2p$ and hybridized Fe unfilled t_{2g} bands [27,28]. In addition, at the interface, the Fe t_{2g} band is situated lower than the Ti band. In the lower carrier concentration region, the conduction electron fills the Fe band, giving a flavor of magnetism and leading to a strong magnetic correlation effect [22,27–30], whereas the disappearance of the anomalous Hall effect and negative MR at high carrier density limit is not clear at this moment. Further spectroscopic study at the interface and detailed band-structure calculation are needed to understand this. We have prepared several other conducting interfaces and performed similar magnetotransport measurements as controlled experiments. Figure 4(d) presents a comparative study of the percent MR of differ-

ent conducting oxide samples (LAO-STO, LaVO$_3$-STO, and Nb-doped STO) and our present LFO-STO interface. The inset of Fig. 4(d) is the enlarged version of the percent MR as a function of B for LAO-STO, LaVO$_3$-STO, and Nb-doped STO samples. A comparative study of the anomalous Hall effect is also shown in Fig. 4(e) as a function of B. The inset presents the raw Hall data as a function of B. It is remarkable to note that both negative MR and anomalous Hall effect at room temperature are unique only to the LFO-STO interface. Figure 4(f) represents the percent transmission of light of the sample as a function of light energy. Around 90% transparency was observed with a negligible drop in transmission above the visible region to the infrared region. The inset of Fig. 4(f) shows a photograph of the sample, indicating the optical transparent nature of the sample.

In conclusion, LFO-STO is found to have a temperature-dependent transition into a regime supporting spin-polarized transport at the interface. Interestingly, the temperature-dependent spin polarization is found to emerge from the structural phase transition associated with the nonmagnetic
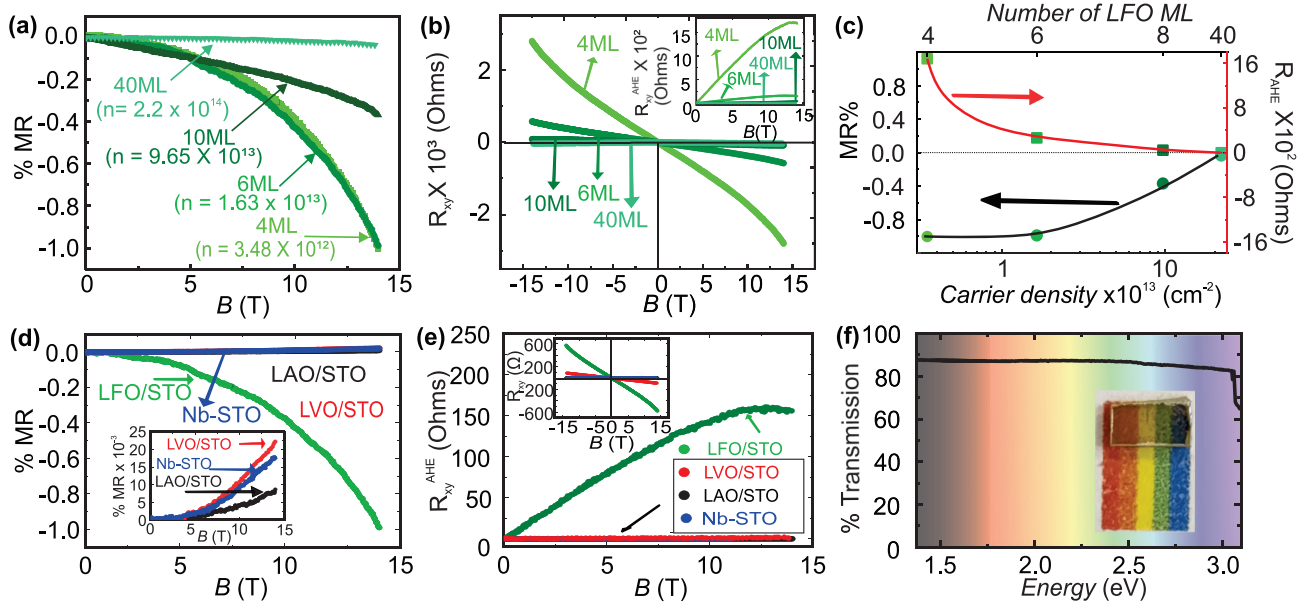
FIG. 4. Magnetotransport measurements for LFO-STO, LVO-STO, LAO-STO, and Nb-STO at 300 K and band schematic for LFO-STO interface. (a) % magnetoresistance (MR) as a function of the applied magnetic field measured at 300 K for conducting interface LFO-STO with different thicknesses of LFO thin films (4, 6, 10, and 40 ml) as mentioned in the figure. (b) Hall resistance as a function of the applied magnetic field measured at 300 K for conducting interface LFO-STO with different thicknesses of LFO thin films (4, 6, 10, and 40 ml) as mentioned in the figure. The inset presents the anomalous part of these samples as a function of the applied magnetic field. (c) % MR (left axis) and anomalous Hall resistance (right axis) as a function of charge carrier density (mentioned at the bottom axis) formed at the conducting interface of LFO-STO with different LFO thicknesses (mentioned at the top axis). (d) % MR as a function of the applied magnetic field measured at 300 K for conducting interface of LAO-STO, LVO-STO, LFO-STO, and Nb-doped single crystal of STO as mentioned in the figure. The inset shows the zoomed version of the same. (e) Anomalous Hall resistance as a function of the applied magnetic field measured at 300 K for conducting interface of LAO-STO, LVO-STO, LFO-STO, and Nb-doped single crystal of STO as mentioned in the figure. The inset shows the raw Hall data without linear subtraction. (f) % transmission of light as a function of light energy. The inset presents the real image of the sample.

STO substrate. Unlike the LAO-STO interface, the unusual spin-polarized transport in the high-temperature regime established here may produce surprising effects that are not only interesting from the point of view of fundamental physics but also could be utilized to realize materials for spin-electronics applications at room temperature. Our result may open an avenue in the field of spintronics to design materials with appropriate electronics band alignment, nontrivial spin texture, and above all, a coupling between them.

[1] J. Mannhart and D. G. Schlom, Oxide interfaces—An opportunity for electronics, Science **327**, 1607 (2010).

[2] H. Y. Hwang, Y. Iwasa, M. Kawasaki, B. Keimer, N. Nagaosa, and Y. Tokura, Emergent phenomena at oxide interfaces, Nat. Mater. **11**, 103 (2012).

[3] N. Nagaosa, J. Sinova, S. Onoda, A. H. MacDonald, and N. P. Ong, Anomalous Hall effect, Rev. Mod. Phys. **82**, 1539 (2010).

[4] M. Diez, A. M. R. V. L. Monteiro, G. Mattoni, E. Cobanera, T. Hyart, E. Mulazimoglu, N. Bovenzi, C. W. J. Beenakker, and A. D. Caviglia, Giant negative magnetoresistance driven by spin-orbit coupling at the LaAlO$_3$/SrTiO$_3$ interface, Phys. Rev. Lett. **115**, 016803 (2015).

[5] N. Wadehra, R. Tomar, R. M. Varma, R. K. Gopal, Y. Singh, S. Dattagupta, and S. Chakraverty, Planar Hall effect and anisotropic magnetoresistance in polar-polar interface of LaVO$_3$-KTaO$_3$ with strong spin-orbit coupling, Nat. Commun. **11**, 874 (2020).

[6] T. Suzuki, L. Savary, J. P. Liu, J. W. Lynn, L. Balents, and J. G. Checkelsky, Singular angular magnetoresistance in a magnetic nodal semimetal, Science **365**, 377 (2019).

[7] S. Bhowal and S. Satpathy, Electric field tuning of the anomalous Hall effect at oxide interfaces, npj Comput. Mater. **5**, 61 (2019).

[8] B. Pang, L. Zhang, Y. B. Chen, J. Zhou, S. Yao, S. Zhang, and Y. Chen, Spin-glass-like behavior and topological Hall effect in

SrRuO$_3$/SrIrO$_3$ superlattices for oxide spintronics applications, ACS Appl. Mater. Interfaces **9**, 3201 (2017).

[9] D. Xiao, W. Zhu, Y. Ran, N. Nagaosa, and S. Okamoto, Interface engineering of quantum Hall effects in digital transition metal oxide heterostructures, Nat. Commun. **2**, 596 (2011).

[10] A. Gupta, H. Silotia, A. Kumari, M. Dumen, S. Goyal, R. Tomar, N. Wadehra, P. Ayyub, and S. Chakraverty, KTaO$_3$—The new kid on the spintronics block, Adv. Mater. **34**, 2106481 (2022).

[11] A. Ohtomo and H. Y. Hwang, A high-mobility electron gas at the LaAlO$_3$/SrTiO$_3$ heterointerface, Nature (London) **427**, 423 (2004).

[12] F. Bi, M. Huang, S. Ryu, H. Lee, C. W. Bark, C. B. Eom, P. Irvin, and J. Levy, Room-temperature electronically-controlled ferromagnetism at the LaAlO$_3$/SrTiO$_3$ interface, Nat. Commun. **5**, 5019 (2014).

[13] N. Kumar, N. Wadehra, R. Tomar, Shama, S. Kumar, Y. Singh, S. Dattagupta, and S. Chakraverty, Observation of Shubnikov–de Haas oscillations, planar Hall effect, and anisotropic magnetoresistance at the conducting interface of EuO–KTaO$_3$, Adv. Quantum Technol. **4**, 2000081 (2021).

[14] S. Tripathi, R. Rana, S. Kumar, P. Pandey, R. S. Singh, and D. S. Rana, Ferromagnetic CaRuO$_3$, Sci. Rep. **4**, 3877 (2014).

[15] E. K. Ko, J. Mun, H. G. Lee, J. Kim, J. Song, S. H. Chang, T. H. Kim, S. B. Chung, M. Kim, L. Wang *et al.*, Oxygen vacancy engineering for highly tunable ferromagnetic properties: A case of SrRuO$_3$ ultrathin film with a SrTiO$_3$ capping layer, Adv. Func. Mater. **30**, 2001486 (2020).

[16] J. S. Kim, S. S. A. Seo, M. F. Chisholm, R. K. Kremer, H.-U. Habermeier, B. Keimer, and H. N. Lee, Nonlinear Hall effect and multichannel conduction in LaTiO$_3$/SrTiO$_3$ superlattices, Phys. Rev. B **82**, 201407(R) (2010).

[17] H. Rotella, O. Copie, A. Pautrat, P. Boullay, A. David, D. Pelloquin, C. Labbé, C. Frilay, and W. Prellier, Kondo effect goes anisotropic in vanadate oxide superlattices, J. Phys. Condens. Matter **27**, 095603 (2015).

[18] J. Luning, F. Nolting, A. Scholl, H. Ohldag, J. W. Seo, J. Fompeyrine, J. P. Locquet, and J. Stohr, Determination of the antiferromagnetic spin axis in epitaxial LaFeO$_3$ films by x-ray magnetic linear dichroism spectroscopy, Phys. Rev. B **67**, 214433 (2003).

[19] J. W. Seo, E. E. Fullerton, F. Nolting, A. Scholl, J. Fompeyrine, and J. P. Locquet, Antiferromagnetic LaFeO$_3$ thin films and their effect on exchange bias, J. Phys. Condens. Matter **20**, 264014 (2008).

[20] P. Xu, W. Han, P. M. Rice, J. Jeong, M. G. Samant, K. Mohseni, H. L. Meyerheim, S. Ostanin, I. V. Maznichenko, I.

Mertig *et al.*, Reversible formation of 2D electron gas at the LaFeO$_3$/SrTiO$_3$ interface via control of oxygen vacancies, Adv. Mater. **29**, 1604447 (2017).

[21] I. V. Maznichenko, S. Ostanin, A. Ernst, J. Henk, and I. Mertig, Formation and tuning of 2D electron gas in perovskite heterostructures, Phys. Status Solidi B **257**, 1900540 (2020).

[22] H. Nishikawa, F. Itani, T. Kawaguchi, H. Tanaka, and N. Iwata, Metallic conductivity of the heterointerface between LaFeO$_3$ and SrTiO$_3$, Solid State Commun. **323**, 114105 (2021).

[23] S. R. Spurgeon, P. V. Sushko, S. A. Chambers, and R. B. Comes, Dynamic interface rearrangement in LaFeO$_3$/n−SrTiO$_3$ heterojunctions, Phys. Rev. Mater. **1**, 063401 (2017).

[24] See Supplemental Material at http://link.aps.org/supplemental/10.1103/PhysRevB.109.L201114 for Fig. S1: (a) Surface characterization and (b) atomic force microscopy image of the STO substrate and LFO thin film grown on STO substrate. (c) RHEED oscillations for 6 ml LFO-STO samples, and the insets depict the RHEED pattern before and after the growth of LFO film on STO. Figure S2: Magnetization as a function of magnetic field for selected temperatures of the LFO thin film on STO (001). Figure S3: (a) and (b) Magnetization measurements and (c) magnetization as a function of temperature for different thicknesses of the LFO thin film on STO (001). Figure S4: $(dR_{xy}/dB)_{B=13T} - (dR_{xy}/dB)_{B=3T}$ as function of temperature for 6 ml LFO-STO interface. Anomalous Hall resistance (right axis) as a function of the temperature of the 6 ml LFO-STO interface. The black and red doted lines are the eye guided lines.

[25] E. McCalla, J. Walter, and C. Leighton, A unified view of the substitution-dependent antiferrodistortive phase transition in SrTiO$_3$, Chem. Mater. **28**, 7973 (2016).

[26] Z. Zhang, P. Qian, X. Yang, B. Wu, H. L. Cai, F. M. Zhang, and X. S. Wu, Manipulating the carrier concentration and phase transition via Nb content in SrTiO$_3$, Sci. Rep. **12**, 2499 (2022).

[27] T. Arima, Y. Tokura, and J. B. Torrance, Variation of optical gaps in perovskite-type $3d$ transition-metal oxides, Phys. Rev. B **48**, 17006 (1993).

[28] R. Comes and S. Chambers, Interface structure, band alignment, and built-in potentials at LaFeO$_3$/n−SrTiO$_3$ heterojunctions, Phys. Rev. Lett. **117**, 226802 (2016).

[29] R. Tomar, N. Wadehra, V. Budhiraja, B. Prakash, and S. Chakraverty, Realization of single terminated surface of perovskite oxide single crystals and their band profile: (LaAlO$_3$)$_{(0.3)}$(Sr$_2$AlTaO$_6$)$_{(0.7)}$, SrTiO$_3$ and KTaO$_3$ case study, Appl. Surf. Sci. **427**, 861 (2018).

[30] T. Jungwirth, Q. Niu, and A. H. MacDonald, Anomalous Hall effect in ferromagnetic semiconductors, Phys. Rev. Lett. **88**, 207208 (2002).